

FULLY ADAPTABLE BAND-STOP FILTER USING VARACTOR DIODES

Carles Musoll-Anguiano,¹ Ignacio Llamas-Garro,¹ Zabdíel Brito-Brito,¹ Lluís Pradell,¹ and Alonso Corona-Chavez²

¹Signal Theory and Communications Department, Technical University of Catalonia, Barcelona 08034, Spain; Corresponding author: llamasi@ieee.org

²National Institute for Astrophysics, Optics and Electronics, Puebla 72840, Mexico

Received 2 June 2009

ABSTRACT: In this article a reconfigurable band-stop filter able to reconfigure center frequency, bandwidth, and selectivity for fine tuning applications is demonstrated, device topology discussion and implementation details are given, and followed by discussion on simulations and measurements. The reconfigurable filter topology has four poles and a quasi-elliptic band-stop filter response. The device is tuned by varactor diodes placed at different locations on the filter; varactors are voltage controlled in pairs due to filter symmetry for center frequency and bandwidth control. An additional varactor is placed on a crossing line to move a pair of transmission zeros, closer or farther to the filter center frequency, which tunes filter selectivity. Simulations show a tuneable center frequency range from 1.42 to 1.48 GHz, a tuneable fractional bandwidth range from 9.46 to 12.96%, and a tuneable selectivity range from 0.53 to 0.65 dB/MHz. Measurements show a tuneable center frequency range from 1.37 to 1.43 GHz, a tuneable fractional bandwidth range from 11.31 to 15.93%, and a selectivity tuning range from 0.37 to 0.40 dB/MHz. Simulations and measurements are in good agreement.

© 2010 Wiley Periodicals, Inc. *Microwave Opt Technol Lett* 52: 554–558, 2010; Published online in Wiley InterScience (www.interscience.wiley.com). DOI 10.1002/mop.24969

Key words: continuously tuned filter; band-stop quasi-elliptic filter; varactor diode; reconfigurable filter; transmission zeros

1. INTRODUCTION

There is an increased demand for microwave filters with advanced features that can make radio frequency (RF) systems much more efficient and adaptable to multiple bands. Reconfigurable filters can reduce the complexity of a system avoiding the introduction of filter banks; the filter presented in this article finds its application in adaptable image rejection receivers. Earlier work has been primarily focused on center frequency or bandwidth control [1–8]. Filter parameters like center frequency or bandwidth can be controlled continuously, discretely, or a combination of both. Continuously tuned filters have been implemented using varactor diodes [9–15], MEMS varactors [16–20], or ferroelectric materials [21–24]. On the other hand, discretely tuned filters have been implemented using PIN diodes [25–31] or MEMS switches [32–34]. The band-stop filter in Ref. [35] uses PIN diodes to control filter center frequency discretely, meanwhile varactor diodes provide a continuous bandwidth reconfiguration at a given frequency. The filter presents discrete center frequencies in the range from 0.5 to 2 GHz, and continuous bandwidth reconfiguration in the range from 30 to 42%. In Ref. [36], a switchable band-stop filter with two different center frequencies is presented; the filter topology allows precise control over frequency and bandwidth discretely, achieved by choosing resonator sections switched by PIN diodes. In this article, we propose selectivity tuning in addition to center frequency and bandwidth reconfigurability, using a quasi-elliptic band-stop filter response; selectivity tuning is achieved in a band-stop filter response for the first time by the authors as compared to previous work in Ref. [1] and [11]. The filter is capable of having

different center frequency states with precise bandwidth control, or alternatively having different fractional bandwidths with a fixed center frequency. Moreover, the filter allows selectivity tuning for each state. All filter parameters are tuned continuously. In this article, a discussion on the filter topology and its implementation, including a thorough comparison between simulations and measurements on filter performance, has been added compared to previous work [37].

2. BAND-STOP FILTER TOPOLOGY

The filter is designed to have a quasi-elliptic band-stop filter response, having one pair of transmission zeros at finite frequencies. The transmission zeros have been achieved by a cross-coupling line between a pair of nonadjacent resonators. The simulated [38] comparison between a Chebyshev and quasi-elliptic filter response is shown in Figure 1. The Chebyshev response is achieved by having a filter topology without the crossing line between nonadjacent resonators [1]. The quasi-elliptic band-stop ladder network of the proposed filter is shown in Figure 2. By varying the coupling capacitances C_i between the main transmission line and each resonator, the bandwidth of the filter can be modified. The series LC models transmission line resonators are loaded by capacitances C_j on one end. By varying C_j , the filter center frequency can be modified. By varying the cross coupling capacitance between nonadjacent resonators, C_k , the filter selectivity can be modified.

The design of the reconfigurable four pole quasi-elliptic band-stop filter starts with a low-pass quasi-elliptic prototype filter [39]. It is well known that an element transformation of the low-pass element values and frequency mapping produces the desired theoretical filter response [39]. Through this method the values of C_i , L , and $C_{\text{resonator}}$ can be determined, where $C_{\text{resonator}} = (C \times C_j)/(C + C_j)$ (Fig. 2). The filter was initially designed to have a center frequency at 1.41 GHz, with a 15% fractional bandwidth. Varactor diodes were then inserted on the filter topology to tune filter parameters. The quasi-elliptic low-pass prototype elements used for the proposed filter are given in Table 1.

In Table 1, Ω_a is the attenuation pole frequency, g_1 and g_2 are the low-pass elements for the first and second resonator of the filter. Only half of the values are given due to filter symmetry. An immittance inverter J_a is located between resonators 2 and 3 (Fig. 2). The immittance inverter J_b corresponds to the

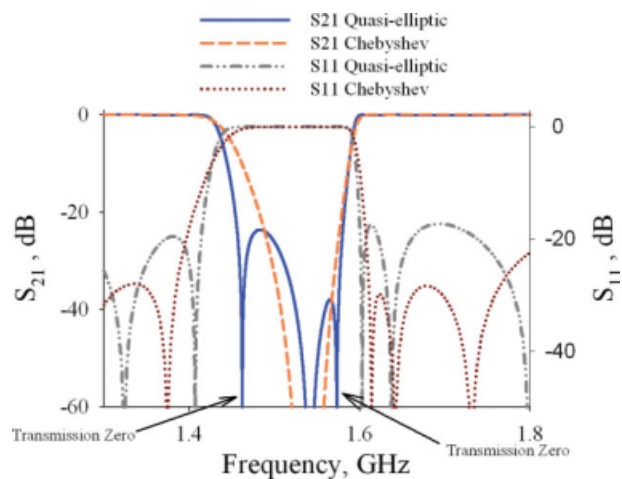


Figure 1 Comparison between a Chebyshev and a quasi-elliptic band-stop filter response. [Color figure can be viewed in the online issue, which is available at www.interscience.wiley.com]

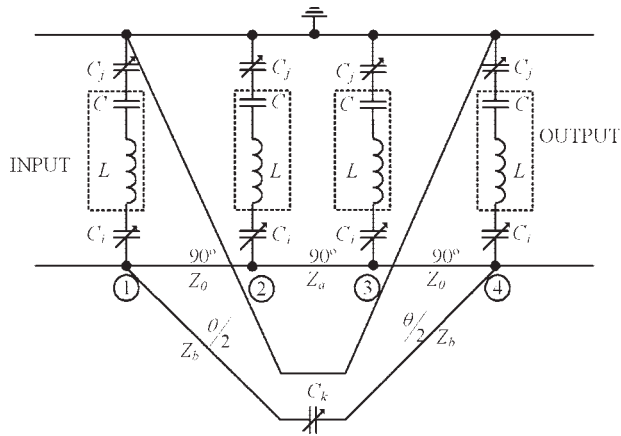


Figure 2 Quasi-elliptic band-stop filter ladder network

cross coupling between nonadjacent resonators 1 and 4 (Fig. 2); J_a and J_b have opposite signs, and hence, the cross coupling line has an electrical length of 270° . From Table 1, the impedance of the line between resonators 2 and 3 in Figure 2 is around 50Ω . Similarly the impedance of the crossing line between resonators 1 and 4 in Figure 2 is found to be $Z_b = 250 \Omega$. As a 250Ω line is impractical for fabrication using conventional photolithography, two $\theta/2$ line sections connected by a series capacitor C_k , as shown in Figure 2 were used instead. To find the value of capacitor C_k , first the line length θ is chosen to give a value of admittance Y_b from (1) that corresponds to a 65Ω impedance line suitable for realization using a conventional photolithographic process. Then, the value of C_k can be calculated using (2), where Z_0 is the characteristic impedance of the line and f_0 is the filter center frequency. Using (2), C_k was calculated to be 0.3pF , where θ in (1) was taken as 120° .

$$Y_b = \frac{J_b}{\tan\left[\frac{\theta}{2}\right]} \quad (1)$$

$$C_k = \frac{J_b}{2\pi f_0 Z_0 \left[1 - \left(\frac{J_b}{Y_b}\right)^2\right]} \quad (2)$$

3. FILTER IMPLEMENTATION

This section describes filter layout implementation, including bias circuitry, details of the surface mount components used, and substrate characteristics. Figure 3 shows the proposed filter topology layout that consists of a main transmission line with four transmission line resonators loaded with varactor diodes C_j on one end; these transmission line resonators correspond to the LC resonator model in Figure 2. Filter center frequency control can be attained by modifying the capacitance value of C_j . These resonators are coupled to the main transmission line through varactor diode C_i destined to control the fractional bandwidth of the filter. Selectivity tuning was achieved by varactor diode C_k in the middle of the crossing line that produces the cross coupling between nonadjacent resonators (Figs. 2 and 3). Changing the capacitance of C_k varies the electrical length of the line and

TABLE 1 Quasi-Elliptic Low-pass Prototype Element Values

Ω_a	g_1	g_2	J_a	J_b
1.85	0.95	1.41	1.10	-0.19

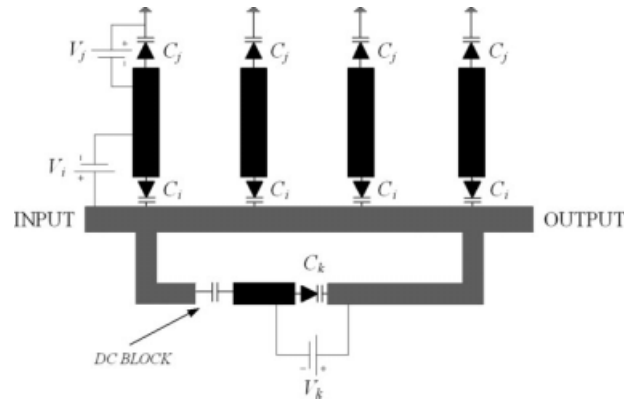


Figure 3 Reconfigurable quasi-elliptic band-stop filter using varactor diodes

hence, the position of the transmission zeros located around the stop-band filter.

The filter was defined photolithographically on a Rogers Duroid substrate ($\epsilon_r = 2.2$ and $\tan\delta = 0.0009$). The RF choke consists of a 177 nF inductor from Tyco Electronics with a self-resonance at 1.7 GHz . The choke inductor has been modeled as a 177 nF inductor in parallel with a 50 fF capacitor. Although the initial filter center frequency is around 1.4 GHz , the inductor isolation is better than -35 dB within the filter operation frequency range. Due to the high isolation of the choke inductor, the microwave signal is not influenced by the DC ports used to provide bias to the active devices.

To prevent a short circuit between the main transmission line and the crossing line, a DC block has been inserted on the crossing line, as shown in Figure 3. The DC block used was a 1 nF capacitor.

Three DC sources in Figure 3 were used to tune the three filter design parameters. V_k controls filter selectivity, V_i controls filter bandwidth, and V_j controls filter center frequency. These DC sources supply the reverse voltage needed to bias the varactor diodes. The grey zone in Figure 3 has positive polarization, and the black one has negative polarization. The varactors were biased using a voltage ranging from 0 to 20 V according to the manufacturer's data sheet.

MACOM varactor diodes MA46470-276 were used for C_k and C_i , and MA4ST402-287 were used for C_j . The MA46470-276 diodes have a capacitance range from 0.3 to 1.8 pF , and the MA4ST402-287 diodes have a capacitance range from 3.86 to 86.29 pF . A photograph of the fabricated filter is shown in Figure 4.

4. RESULTS

This section contains simulated and measured results obtained from the proposed filter. The section is divided into three parts; Section 4.1 shows the results for center frequency tuning. Section 4.2 describes the results for bandwidth tuning. Finally, Section 4.3 shows the results obtained when selectivity is tuned. Simulated results were obtained using commercial software [38] to do electromagnetic simulations taking into account the surface mount component's lumped element models. All measurements were done after a short-open-load-thru calibration, setting the measurement reference plane at the SMA coaxial connectors used to interface the filter with the measurement equipment. Scattering parameters were measured using an Agilent 8510C network analyzer, DC bias was supplied by two Promax FAC-662B power supplies.

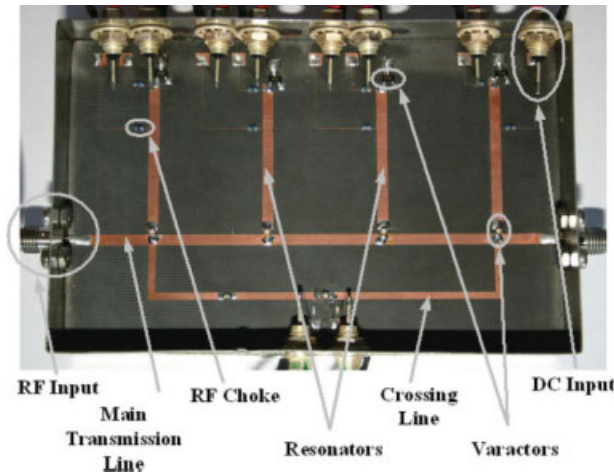


Figure 4 Photograph of the reconfigurable quasi-elliptic band-stop filter. [Color figure can be viewed in the online issue, which is available at www.interscience.wiley.com]

4.1. Center Frequency Tuning

In simulations [38], C_k was fixed to 0.35 pF and C_i was fixed to 1.1 pF to tune filter center frequency. To tune filter center frequency, the capacitances of varactor diodes C_j were varied from 5.6 to 8.1 pF. A center frequency tuning of 60 MHz was achieved within this capacitance range, as shown in the upper part of Figure 5.

To obtain the filter tuneable center frequency, the reverse voltage V_k was fixed to 15 V, V_i was fixed to 2 V, and V_j varied between 16 and 21 V. The varactor diodes C_j were reverse-biased by V_j , which adjusts the resonator electrical lengths to produce the reconfigurable filter center frequency as shown in the lower part of Figure 5. The center frequency is tuned from 1.37 to 1.43 GHz using bias voltages from 16 to 21 V, respectively. A comparison between simulated and measured responses of the filter when tuning filter center frequency is shown in Table 2, where a very good agreement between simulations and measurements was obtained.

4.2. Bandwidth Tuning

In simulations [38], bandwidth tuning was controlled by C_i , which modifies the resonator capacitive coupling from the main transmission line. This produces an additional variation of filter

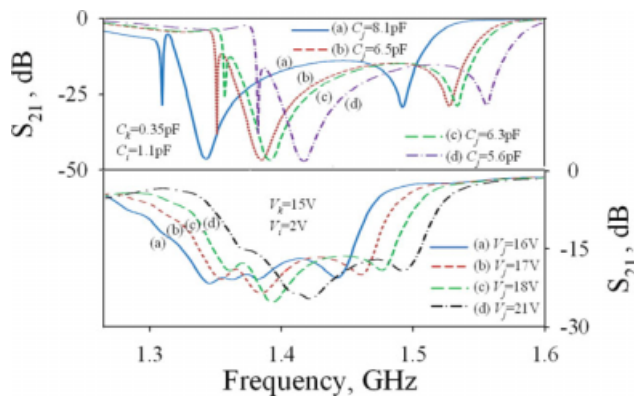


Figure 5 Simulated and measured results for the band-stop filter with center frequency control (upper part: simulated response, lower part: measured response). [Color figure can be viewed in the online issue, which is available at www.interscience.wiley.com]

TABLE 2 Comparison Between Simulation and Measurement Results for Filter Centre Frequency Tuning

State	Simulation		Measurement	
	f_0 (GHz)	FBW(%)	f_0 (GHz)	FBW(%)
(a)	1.42	14.31	1.37	15.54
(b)	1.45	14.10	1.39	15.56
(c)	1.46	13.98	1.41	14.92
(d)	1.48	13.62	1.43	13.63
	f_0 range tuning: 60 MHz		f_0 range tuning: 60 MHz	

center frequency, due to the fact that varying C_i will slightly capacitively load the resonators. Therefore, C_j was slightly modified to readjust the electrical length of the resonators to provide a fixed filter center frequency at 1.46 GHz, while filter bandwidth was tuned. In simulations, C_i varied between 0.8 and 1.1 pF to reach a fractional bandwidth range from 9.46 to 12.93%, C_k was fixed to 0.35 pF for all states. The simulated response for the filter is shown in the upper part of Figure 6.

In the measurement setup, V_i and V_j were varied simultaneously, whereas V_k is fixed to 15 V. V_i sets the capacitance of C_i using a reverse voltage ranging from 2 to 5 V. Simultaneously, the DC source V_j adjusts the capacitance of C_j using a reverse voltage ranging from 14.1 to 20 V to maintain a fixed filter center frequency. The lower part of Figure 6 shows the measured response for the filter when bandwidth is tuned. The tuneable fractional bandwidth obtained for the filter ranges from 11.31 to 15.93%.

A comparison between simulations and measurements for filter bandwidth tuning is given in Table 3, where a very good agreement between simulations and measurements was obtained.

4.3. Selectivity Tuning

The simulated [38] response when tuning selectivity for the filter is shown in the upper part of Figure 7. First, bandwidth and center frequency are fixed, maintaining $C_i = 1.1$ pF and $C_j = 5.8$ pF and then different values of selectivity are taken by varying the capacitance of varactor diode C_k from 0.3 to 0.6 pF. Selectivity tuning is independent from the other design parameters. To calculate the selectivity for each filter state, we have taken the slope at the most linear part of the filter response in the passband to stopband transition region. The most linear region

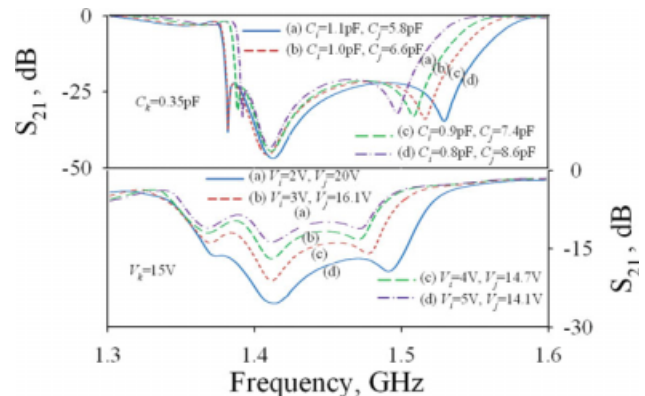


Figure 6 Simulated and measured results for the band-stop filter with stopband bandwidth control (upper part: simulated response, lower part: measured response). [Color figure can be viewed in the online issue, which is available at www.interscience.wiley.com]

TABLE 3 Comparison between Simulation and Measurement Results for Filter Bandwidth Tuning

State	Simulation		Measurement	
	FBW(%)	f_0 (GHz)	FBW(%)	f_0 (GHz)
(a)	12.96	1.47	15.93	1.43
(b)	11.86	1.46	13.29	1.42
(c)	10.65	1.46	11.97	1.42
(d)	9.46	1.46	11.31	1.42
	Total fractional bandwidth variation: 3.50%		Total fractional bandwidth variation: 4.62%	

was found to be between -5 and -10 dB. A selectivity tuning range from 0.53 to 0.65 dB/MHz has been obtained.

In the lower part of Figure 7, filter selectivity tuning measurements are shown. The most linear part of the filter response in the passband to stopband transition was chosen to calculate the slope and found to be between -5 and -10 dB. Varactor diode C_k is reverse-biased by V_k to produce a selectivity variation from 0.37 to 0.40 dB/MHz, whereas V_i and V_j are fixed to 2 and 20 V, respectively. The reverse voltage of V_k ranges from 2 to 20 V. A higher variation in selectivity was observed when the bias voltage values were in the range from 15 to 20 V. Within these voltage bias values, the capacitance of the varactor diode is smaller. Therefore, as the reverse voltage increases, the capacitance values decrease and filter selectivity becomes lower. Table 4 contains a comparison of simulated and measured results for selectivity tuning. The measured selectivity tuning range was limited by the parasitic capacitance of the varactor diode mount, including solder pads and solder that added up to the varactor diode C_k capacitance; this displaced the overall capacitance value outside the values that would give a maximum selectivity tuning. Although selectivity tuning has been successfully demonstrated, higher values of measured selectivity tuning can be obtained by accurately modeling the varactor diode mount to account for capacitive parasitic effects that can affect the overall value of C_k calculated from (2).

5. CONCLUSIONS

A reconfigurable band-stop filter with a pair of transmission zeros has been proposed and successfully demonstrated. A careful comparison between simulations and measurements has been carried out to validate the design theory and implementation. Se-

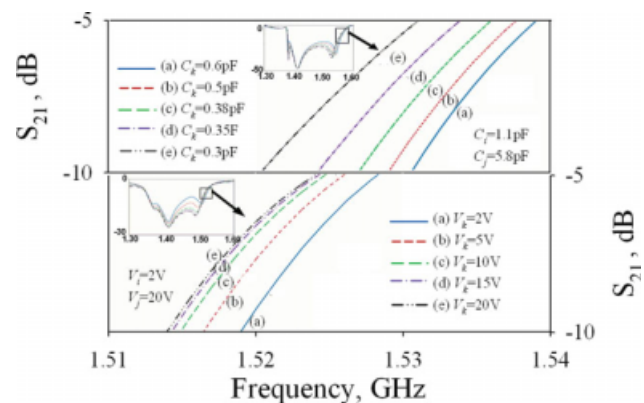


Figure 7 Simulated and measured results for the band-stop filter with selectivity control (upper part: simulated response, lower part: measured response). [Color figure can be viewed in the online issue, which is available at www.interscience.wiley.com]

TABLE 4 Comparison between Simulation and Measurement Result for Filter Selectivity Tuning

State	Simulation	Measurement
	Sel. (dB/MHz)	Sel. (dB/MHz)
(a)	0.65	0.40
(b)	0.64	0.39
(c)	0.63	0.38
(d)	0.58	0.38
(e)	0.53	0.37
	Selectivity tuning range: 0.12 dB/MHz	Selectivity tuning range: 0.03 dB/MHz

lectivity tuning for the filter has been obtained by varying the capacitance of a varactor diode situated on the crossing line that produces the cross-coupled circuit. Bandwidth tuning has been controlled by varactor diodes used to couple resonators to the main transmission line. The center frequency of the filter is controlled by varactor diodes placed at the end of transmission line resonators. The filter topology presented in this article is able to tune all filter design parameters continuously and can be perfectly adjusted to produce a fractional bandwidth range from 11.51 to 15.46%, a center frequency range from 1.34 to 1.42 GHz, and a selectivity tuning range from 0.37 to 0.40 dB/MHz.

ACKNOWLEDGMENTS

This work has been financed by research project TEC2007-65705/TCM from the Spanish Ministry of Education and Culture.

REFERENCES

1. I.C. Hunter and J.D. Rhodes, Electronically tunable microwave bandstop filters, *IEEE Trans Microwave Theory Tech* 30 (1982), 1361–1367.
2. S.R. Chandler, I.C. Hunter, and J.G. Gardiner, Active varactor tunable microwave filters, *Proceedings of 23rd European Microwave Conference*, 1993, pp. 244–245.
3. H. Uchida, A. Sato, A. Ohno, N. Yoneda, Y. Konishi, and S. Makino, A widely-tunable balanced bandstop filter with low reflections and separate stop-bands, *Proceedings of Asia-Pacific Microwave Conference*, 2006, Yokohama, Japan, pp. 641–644.
4. X.-H. Wang, B.-Z. Wang, H. Zhang, and K.J. Chen, A tunable bandstop resonator based on a compact slotted ground structure, *IEEE Trans Microwave Theory Tech* 55 (2007), 1912–1918.
5. W.D. Yan and R.R. Mansour, Compact tunable bandstop filter integrated with large deflected actuators, *IEEE MTT-S International Microwave Symposium*, Honolulu, HI, 2007, pp. 1611–1614.
6. M.F. Karim, A.Q. Liu, A.B. Yu, and A. Alphones, MEMS-based tunable bandstop filter using electromagnetic bandgap (EBG) structures, *Proc Asia-Pacific Microwave Conf* 3 (2005), 4.
7. G. Zheng and J. Papapolymerou, Monolithic reconfigurable band-stop filter using RF MEMS switches, *Int J RF Microwave Comput Aided Eng* 14 (2004), 373–382.
8. A. Takacs, D. Neculoiu, D. Vasilache, A. Muller, P. Pons, H. Aubert, and R. Plana, Tunable MEMS filters for millimeter wave applications, *Proc Int Semiconductor Conf* 1 (2006), 115–118.
9. C.-K. Liao, C.-Y. Chang, and J. Lin, A reconfigurable filter based on doublet configuration, *IEEE MTT-S International Microwave Symposium*, Honolulu, HI, 2007, pp. 1607–1610.
10. M.-S. Chung, I.-S. Kim, and S.-W. Yun, Varactor-tuned hairpin bandpass filter with an attenuation pole, *Proc Asia-Pacific Microwave Conf* 4 (2005), 4.
11. I.C. Hunter and J.D. Rhodes, Electronically tunable microwave bandpass filters, *IEEE Trans Microwave Theory Tech* 9 (1982), 1354–1360.

12. M. Sanchez-Renedo, R. Gomez-Garcia, J.I. Alonso, and C. Briso-Rodriguez, Tunable combline filter with continuous control of center frequency and bandwidth, *IEEE Trans Microwave Theory Tech* 53 (2005), 191–199.
13. M. Makimoto and M. Sagawa, Varactor tuned bandpass filters using microstrip-line ring resonators, *IEEE MTT-S Int Microwave Symp* 86 (1986), 411–414.
14. A.R. Brown and G.M. Rebeiz, A varactor-tuned RF filter, *IEEE Trans Microwave Theory Tech* 48 (2000), 1157–1160.
15. X.-P. Liang and Y. Zhu, Hybrid resonator microstrip line electrically tunable filter, *IEEE MTT-S Int Microwave Symp* 3 (2001), 1457–1460.
16. A. Abbaspour-Tamijani, L. Dussopt, and G.M. Rebeiz, Miniature and tunable filters using MEMS capacitors, *IEEE Trans Microwave Theory Tech* 51 (2003), 1878–1885.
17. E. Fourn, C. Quendo, E. Rius, A. Pothier, P. Blondy, C. Champeaux, J.C. Orlianges, A. Catherinot, G. Tanne, C. Person, and F. Huret, Bandwidth and central frequency control on tunable bandpass filter by using MEMS cantilevers, *IEEE MTT-S Int Microwave Symp* 1 (2003), 523–526.
18. D. Mercier, J.-C. Orlianges, T. Delage, C. Champeaux, A. Catherinot, D. Cros, and P. Blondy, Millimeter-wave tune-all bandpass filters, *IEEE Trans Microwave Theory Tech* 52 (2004), 1175–1181.
19. J.-M. Kim, S. Lee, J.-H. Park, J.-M. Kim, C.-W. Baek, Y. Kwon, and Y.-K. Kim, Low loss K-band tunable bandpass filter using micromachined variable capacitors, *Proc Int Conf on Solid-State Sensors, Actuators Microsyst* 1 (2005), 1071–1074.
20. M.J. Prest, Y. Wang, F. Huang, and M.J. Lancaster, Silicon combdrive actuators for low-temperature tuning of superconducting microwave circuits, *J Micromech Microeng* 18 (2008), 7.
21. Y.-H. Chun, J.-S. Hong, P. Bao, T.J. Jackson, and M.J. Lancaster, BST varactor tuned bandstop filter with slotted ground structure, *IEEE MTT-S International Microwave Symposium, Atlanta, GA, 2008*, pp. 1115–1118.
22. G. Sanderson, A.H. Cardona, T.C. Watson, D. Chase, M.M. Roy, J.M. Paricka, and R.A. York, Tunable IF filter using thin-film BST varactors, *IEEE MTT-S International Microwave Symposium, 2007*, pp. 679–682.
23. J. Nath, D. Ghosh, J.-P. Maria, A.I. Kingon, W. Fathelbab, P.D. Franzone, and M.B. Steer, An electronically tunable microstrip bandpass filter using thin-film Barium-Strontium-Titanate (BST) varactors, *IEEE Trans Microwave Theory Tech* 53 (2005), 2707–2712.
24. Y.-H. Chun, J.-S. Hong, P. Bao, T.J. Jackson, and M.J. Lancaster, BST-varactor tunable dual-mode filter using variable zc transmission line, *IEEE Microwave Wireless Compon Lett* 18 (2008), 167–169.
25. C. Lugo and J. Papapolymerou, Electronic switchable bandpass filter using PIN diodes for wireless low cost system-on-a-package applications *IEEE Proc Microwave Antennas Propag* 151 (2004), 497–502.
26. M. Koochakzadeh and A. Abbaspour-Tamijani, Switchable bandpass filter for 0.3–0.6 GHz, *IEEE MTT-S International Microwave Symposium, 2007*, pp. 557–560.
27. C. Rauscher, Reconfigurable bandpass filter with a three-to-one switchable passband width, *IEEE Trans Microwave Theory Tech* 51 (2003), 573–577.
28. C. Lugo and J. Papapolymerou, Six-state reconfigurable filter structure for antenna based systems, *IEEE Trans Antennas Propag* 54 (Part 1), (2006), 479–483.
29. F. Mahe, G. Tanne, E. Rius, C. Person, S. Toutain, F. Biron, L. Billonnet, B. Jarry, and P. Guillon, Electronically switchable dual-band microstrip interdigital bandpass filter for multistandard communication applications, *Proceedings of the 30th European Microwave Conference, Paris, France, October 2000*, 4 pp.
30. C. Lugo and J. Papapolymerou, Single switch reconfigurable bandpass filter with variable bandwidth using a dual-mode triangular patch resonator, *IEEE MTT-S International Microwave Symposium, Long Beach, CA, 2005*, pp. 779–782.
31. C. Lugo, J. Hadrick, and J. Papapolymerou, Dual mode reconfigurable filter for 3d system on package (SOP) integration, *Proceedings of the 55th Electronic Components and Technology Conference, 2005*, pp. 532–535.
32. C.D. Nordquist, C.L. Goldsmith, C.W. Dyck, G.M. Kraus, P.S. Finnegan, F. Austin, and C.T. Sullivan, X-band RF MEMS tuned combline filter, *Electron Lett* 41 (2005), 76–77.
33. C.D. Nordquist, A. Muyschondt, M.V. Pack, P.S. Finnegan, C.W. Dyck, I.C. Reines, G.M. Kraus, T.A. Plut, G.R. Sloan, C.L. Goldsmith, and C.T. Sullivan, An X-band to Ku-band RF MEMS switched coplanar strip filter, *IEEE Microwave Wireless Compon Lett* 14 (2004), 425–427.
34. A. Ocera, P. Farinelli, P. Mezzanotte, R. Sorrentino, B. Margesin, and F. Giacomozzi, A novel MEMS-tunable hairpin line filter on silicon substrate, *Proceedings of the 36th European Microwave Conference, Manchester, England, 2006*, pp. 803–806.
35. B.E. Carey-Smith and P.A. Warr, Broadband-configurable bandstop-filter design employing a composite tuning mechanism, *IET Proc Microwave Antennas and Propag* 1 (2007), 420–426.
36. Z. Brito-Brito, I. Llamas-Garro, L. Pradell, and A. Corona-Chavez, Microstrip switchable bandstop filter using PIN Diodes with Precise frequency and bandwidth control, *Proceedings of the 38th European Microwave Conference Amsterdam, The Netherlands, 28–30 October 2008*, pp. 1707–1710.
37. C. Musoll-Anguiano, I. Llamas-Garro, Z. Brito-Brito, L. Pradell, and A. Corona-Chavez, Characterizing a tune all bandstop filter, *IEEE MTT-S Int Microwave Workshop Series on Signal Integrity and High-Speed Interconnects, Guadalajara, Mexico, 19–20 February 2009*, 4 p.
38. Advanced Design System. Available at: <http://www.agilent.com>.
39. J.-S. Hong and M.J. Lancaster, *Microstrip filters for RF/microwave applications*, Wiley, 2001.

© 2010 Wiley Periodicals, Inc.

WIDEBAND CROSS-COUPLED FILTER USING DEFECTED STEPPED IMPEDANCE RESONATOR

Bian Wu, Xin Lai, Tao Su, and Chang-Hong Liang

School of Electronic Engineering, Xidian University, Xi'an, Shaanxi 710071, People's Republic of China; Corresponding author: bwu@mail.xidian.edu.cn

Received 4 June 2009

ABSTRACT: A novel wideband cross-coupled band-pass filter based on defected stepped impedance resonator (DSIR) is presented in this article. Although the DSIR has opposite impedance characteristic and field distribution to the microstrip SIR, its resonant property is similar to the latter. The internal coupling coefficients of DSIRs are found to be large enough for the wideband filter design. A four-pole, cross-coupled band-pass filter with $f_0 = 1.6$ GHz and $FBW = 12\%$ is designed and fabricated using the folded DSIR. Experimental result has good agreement with the simulation. © 2010 Wiley Periodicals, Inc. *Microwave Opt Technol Lett* 52: 558–561, 2010; Published online in Wiley InterScience (www.interscience.wiley.com). DOI 10.1002/mop.24972

Key words: defected stepped impedance resonator (DSIR); wideband; cross-coupled; band-pass filter (BPF)

1. INTRODUCTION

Recent development in wireless communication system has created a need of band-pass filters with low insertion loss as well as high out-of-band rejection. Cross-coupled filters are widely investigated because they introduce one or more additional couplings between nonadjacent resonators and create finite transmission zeros out of the passband [1, 2]. Furthermore, high data-